

Received August 26, 2018, accepted September 26, 2018, date of publication November 9, 2018, date of current version December 3, 2018.

Digital Object Identifier 10.1109/ACCESS.2018.2879050

# Hybrid Chipless RFID Tags- A Pathway to EPC Global Standard

FATEMEH BABAEIAN<sup>1</sup>, (Student Member, IEEE), AND  
NEMAI CHANDRA KARMAKAR, (Senior Member, IEEE)

Department of Electrical and Computer Systems Engineering, Monash University, Melbourne, VIC 3800, Australia

Corresponding author: Fatemeh Babaeian (fatemeh.babaeian@monash.edu)

This work was supported by the Australian Research Council Link Project—Discreet Reading of Printable Multi-Bit Chipless RFID Tags on Polymer Banknotes—under Grant LP130101044.

**ABSTRACT** Radio frequency identification (RFID) is one of the most modern technologies in identification and tracking systems. Recently, chipless RFID tags have been invented as a low cost, robust, and adaptive alternative, in order to compete with the traditional barcodes identification. However, due to the passive structure, there are a few drawbacks for chipless RFID tags such as short reading range and limitation of encoding data capacity for chipless RFID tags. Hybrid chipless RFID tags have been invented to cope with the limitation of encoding data capacity. This paper reviews the most recent study on hybrid chipless RFID tags and presents an original work on designing a hybrid chipless RFID tag. A novel 3D encoding technique—frequency, polarisation diversity, and frequency division multiplexing—for chipless RFID tags is proposed. The proposed tag encoding data capacity has increased to  $2^{9N}$ , as compared to  $2^{2N}$  in the conventional hybrid tags that were reported prior to this study.

**INDEX TERMS** Hybrid chipless RFID tags, encoding technique, data capacity, radio cross section (RCS), frequency response, resonance, dual band, polarization, frequency division.

## I. INTRODUCTION

RFID is a wireless data capturing technique which uses electromagnetic wave for automatic identification [1]. RFID systems consist of three main elements: a transponder or RFID tag for carrying identification code; an integrator for sending signals to RFID tag, receiving the scattered signal and identifying the ID; and middleware software which maintains an interface to encode identification data from the reader to a personal computer [2]. RFID tags can be categorized into three groups, which are active, semi-active and passive RFID systems. An active transponder requires a power supply which is either a permanent power source or a battery for processing the signal and transmitting the processed signal to the reader. Therefore, an active RFID tag could provide a long reading zone. Semi-active tags have a battery supply which provides power only for signal processing. So in this case, the reading range will be shorter than the active tags. However, passive tags do not require any power supply, and they utilise the EM wave as a source of energy for processing the data and corresponding to the reader. Consequently, the range of detection for passive tags is limited [3].

Although chipped RFID systems have high encoding data capacities and long tag detection ranges, the high price for this technology (10 cents) is a barrier to the utilisation of it in most of the applications. In addition, the lifetime of active tags is

limited. Also, the non-planar structure of classical RFID tags with antenna and chip, and the procedure of fabrication of chipped tags are the main challenges to compete with optical barcode technology for commercial applications. Thus, chipless RFID with passive tags which can be fully printable on different materials have been introduced. Moreover, due to the low cost of printed tags, and non-line of sight tag detection properties, chipless RFID technology is a suitable candidate for the replacement of the conventional barcodes. However, chipless RFID has a few drawbacks, which includes the non-rewritable feature, a shorter range of detection, limitations of encoding data capacity, and the complexity of reading tags.

Chipless RFID tags can be classified into four groups according to their encoding techniques [4]. They are time domain tags [5], [6], frequency domain tags [7], [8], image base tags [9] and hybrid tags. Data can be encoded in chipless RFID tag based on a different electromagnetic aspects of the tag which can be frequency, time, amplitude, phase or polarisation (Fig. 1).

In order to improve the performance of the chipless RFID designs, it is required to have smart designs in the sense of reducing the allocated bandwidth, which is called spectral efficiency, as well as increasing the number of bits per occupied space, known as spatial efficiency. Moreover, by assigning a higher number of bit per each resonator, the chipless

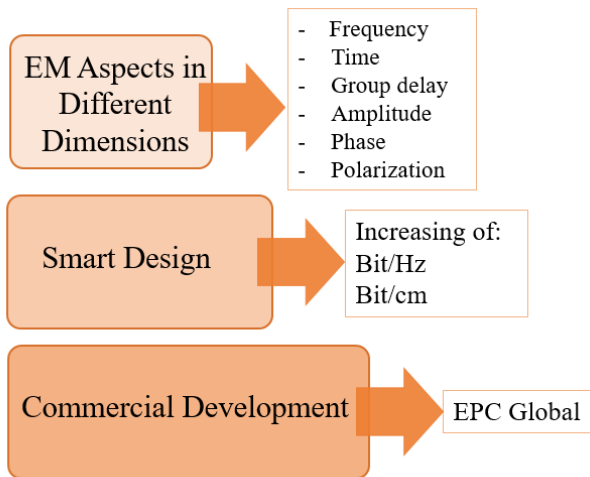


FIGURE 1. Developing chipless RFID tags toward EPC global.

RFID tag can be designed more efficiently. The next stage of designing the smart tag is to enhance its performance and compatibility according to industrial specifications in order to commercialise the technology. For instance, the Electronic Product Code™ (EPC) global standard demands chipless RFID technology to achieve 64 bits data capacity [10]. Therefore, at the design level, increasing data capacity of chipless RFID tags is one of the most crucial challenges that has attracted so many researchers' attention.

There are different types of encoding techniques. Most of them use only one dimension or electromagnetic (EM) parameter of the resonator, which produces only two states of data per resonator. For example, in the frequency-domain-based chipless RFID, only the presence or absence of resonance in a specific frequency defines the code of 0 or 1 in the tag ID [11]. In some of the frequency domain chipless RFID tags data are encoded in both amplitude and phase of frequency response while there is still one bit of information that can be achieved per each element [12]–[15]. Another example of one-dimensional data encoding is embedding data only in group delay, as proposed in [16].

It is clear that using only one dimension of data encoding limits the amount of information encoded by each element. On the other hand, for encoding more information in a single dimension tag, multiple elements are required. Increasing the number of resonators increases the size of chipless RFID tag and makes it impractical for most of the applications [4]. Besides that, there is a maximum number of resonances that can be fit in a specified bandwidth, and increasing operating bandwidth is not always possible as it has the cost of designing UWB reader with a wider bandwidth.

A new approach to increase encoding data capacity is to use hybrid techniques which consider more than one parameter for each unit cell or utilise more than one dimension for data encoding in a given resonator. Therefore, more than one bit of data can be encoded by one element structure. Another approach to increase encoding capacity is to use modulation-encoding methods.

This paper reviews the most recent developments of chipless RFID tag designs. The hybrid tags have multi-dimensional data encoding capability and hence offer higher data capacity than the conventional chipless RFID tags. This paper analyses and classifies the reported hybrid tag into a systematic classification of different hybrid dimensions based on the encoding techniques. Finally, the analytical findings are synthesized in our work of a multi-dimensional hybrid domain chipless RFID for high spectral and spatial efficiencies.

The paper is organized as follows:

Section II introduces different hybrid chipless RFID tags and provides a classification of tags based on encoding techniques. For each type of hybrid tag, the concept will be explained with examples from recent research outcomes.

In section III, we propose a novel hybrid chipless RFID tag with three-dimensional encoding techniques. For this chipless RFID tag, a dual-band resonator with polarisation diversity in the second band is used as well as utilising frequency deviation for increasing data capacity. One of the advantages of this design is that the number of active resonances in the operating bandwidth has been reduced, which can be beneficial in the simplification of the tag ID detection algorithm. Moreover, the structure is designed with a high RCS level, which makes this structure suitable for applications that require tag reading in far distances.

Section IV compares the performance of the proposed three-dimensional chipless RFID tag with the reviewed designs in section II which presents two-dimensional encoding techniques. In this section, the spectral and spatial efficiencies of different encoding techniques reported in the literature are analysed. Finally, section V concludes the paper.

## II. HYBRID CHIPLESS RFID TAGS

As it was mentioned before, in a hybrid chipless RFID tag, more than one dimension is utilised to encode data. It is a goal in hybrid chipless RFID tag to encode data in each dimension independently. As a result, each resonator can produce more than one bit of data. All recently published research in chipless RFID tags can be categorized into five groups according to the method of encoding. These are phase-frequency, polarisation-frequency, time-frequency-group delay based, time-frequency non-group delay-based and modulation based, as demonstrated in Fig. 2. In the next Section, the main concepts of each type of hybrid chipless RFID tag will be explained, and the examples from the recent publication will be discussed.

### A. PHASE-FREQUENCY CHIPLESS RFID TAGS

In a phase-frequency based chipless RFID tag, data are encoded by taking amplitude and phase of the frequency response into consideration. In this encoding technique, one dimension of encoding is related to frequency position, and another dimension is based on the phase derivation. Therefore, structures with sensitive parameters to phase are suitable candidates to be used for this method of encoding. The recent

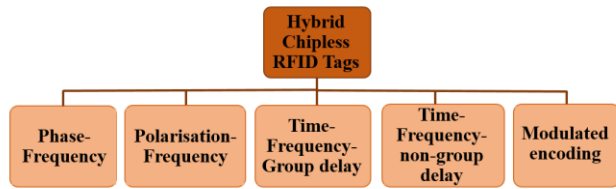


FIGURE 2. Different types of chipless RFID tags.

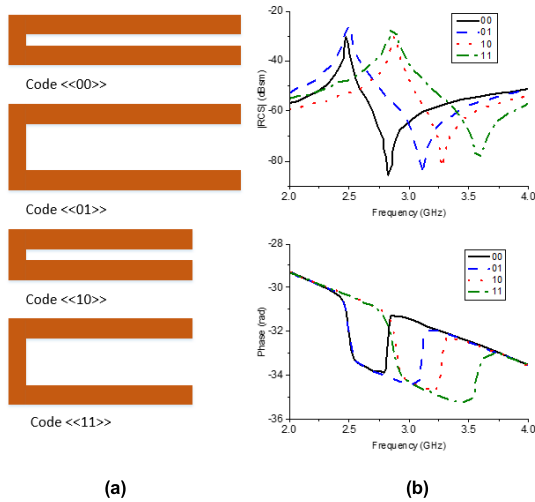


FIGURE 3. (a) C-section hybrid chipless RFID tag. (b) coding principal using phase and frequency shift encoding [17].

studies in phase-frequency encoding in chipless RFID will be discussed in this section.

One of the approaches for encoding data in phase-frequency dimensions is to control the bandwidth of phase and amplitude of RCS in frequency responses. Phase deviation, and frequency selection encoding techniques were proposed by Vena *et al.* [17], in which five C-section resonators were used to achieve 22.9 bits of data. The occupied size of this tag was 2cm × 4cm including five resonators, as shown in Fig. 3 (a). Variation of lengths and gap sizes in C-section resonator shifted the frequency position and changed the shape of phase respectively. As it can be seen in Fig. 3 (b), in each resonance, the dip and peak of frequency could be controlled independently by tuning the length of the resonator and the gap size. Thus, a different phase shape was created at each frequency position. In this work, four possible gap sizes were used to create four phase deviation states for each resonator. It is demonstrated that by using two independent parameters, (frequency position and phase shape), two dimensions of encoding can be allocated to each resonator. The measurement of tag RCS was carried on in a distance of 45cm.

Another phase-frequency encoded chipless RFID transponder was proposed by Balbin and Karmakar [18] in which three square-stub loaded microstrip patch antennas with loading stubs were used, as shown in Fig. 4. In this encoding technique, changing the length of a loaded open circuit stub

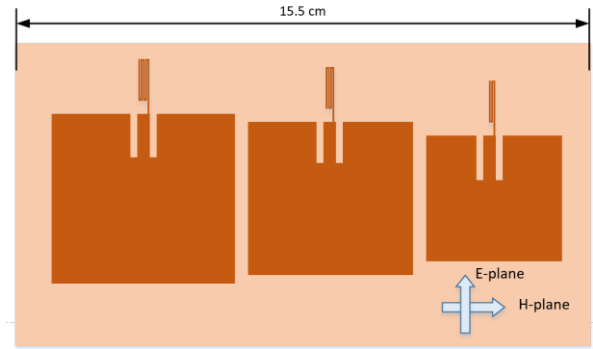


FIGURE 4. Phase coded chipless RFID tag which consists of three patch antennas connected with three meandered open circuit stubs [18].

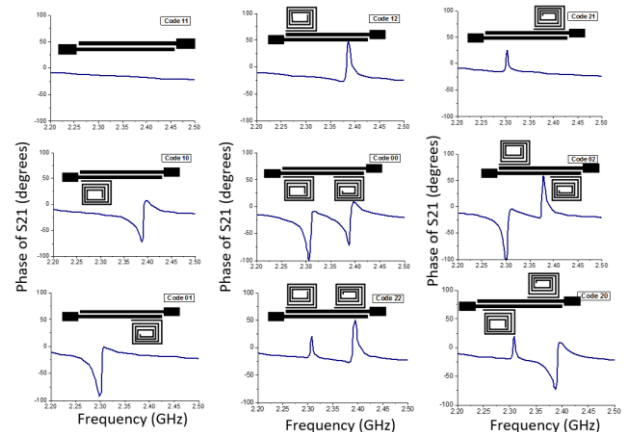


FIGURE 5. The simulated phase response of every nine states of a tag using two Polarization-frequency tags [19].

changed the phase of the backscattered signal in a predicted way, which produced different states of data. It was claimed to have a possible capacity of 108 states of data with a 5-degree resolution of phase in 2.1-2.6GHz while in practice a tag with only two states of data per resonator using 30-degree phase resolution was presented. The structure of this tag was planar and could be printed on low-cost plastic or paper, but the large size of this tag (more than 15 cm for three resonators) was a barrier to most of the applications.

Moreover, a phase encoding method in chipless RFID was proposed by Majidfar *et al.* [19] using a combination of spiral resonators, coupled transmission line and two separated circular wideband monopole antennas as a chipless RFID tag. In this design, as shown in Fig. 5, according to phase shape in three different design variations, three states of code could be produced in each frequency position. The design variations are (1) the absence of resonator, (2) placing the spiral resonator above the transmission line, and (3) placing the spiral resonator below the coupled transmission lines. The main advantages of this tag design were to provide a narrowband response of resonance and a simple encoding method, which is low cost and printable. However, the drawback of this structure was the big size of the tag including the antennas in

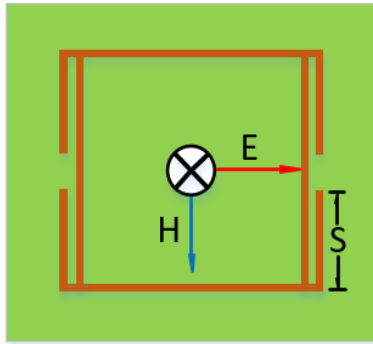


FIGURE 6. Top view of a single unit cell [21].

the structure. The diameters of the antennas are  $D1 = 60$  mm,  $D2 = 90$  mm. Therefore, based on the large size of the tag, this tag cannot be utilised for the applications in which a compact size is needed.

Similarly, Genovesi and Monorchio [20], [21] proposed a phase quantisation encoding on multi-frequency resonators by using the quantised difference between TE and TM phase responses of the tag. In this work, a set of periodic rectangular loop resonators with four stubs attached to each loop corner was used, as shown in Fig. 6. The varying length of those stubs (S) led to a change of the phase response of TE incident wave while the phase response of TM mode was almost unchanged. By calculating the difference between the phases in TE and TM modes and quantising it, different states of data could be achieved. Moreover, in order to guarantee a less steep phase response and increased discrete-phase state, a low dielectric permittivity (Teflon) was used. As a result of using a structure with four ring resonators and phase quantisation of  $\Delta = 10^\circ$ , a maximum of 13.67 bits of data were achieved. The advantages of this tag design were the compact size and its ability to operate in the very narrow frequency band. In addition, in their study, there was an investigation to confirm the independency of phase response for adjacent elements over changing stub length of only one resonator.

### B. POLARISATION-FREQUENCY CHIPLESS RFID TAGS

Encoding in polarisation-frequency based chipless RFID tags is based on using structures which produce different frequency signature when the polarisation of the incident wave varies. In this case, the tag ID code can be created in both frequency and polarisation independently.

In [22], three split ring resonators with polarisation diversity and variable gap configuration were used to encode data. By using this structure, which was very sensitive to the polarisation angle. As shown in Fig. 7, detection of the rotation angle of the tag was possible by resolution of  $20^\circ$ . Each rotation of gap on ring resonator was directly related to the polarisation angle. Thus, according to the place of the gap in each ring and incident wave polarisation angle, different codes in the frequency domain could be produced. To avoid confusion in detection of rotated tag, a ring with a gap in  $0^\circ$  was added as a reference of rotation. It was claimed that

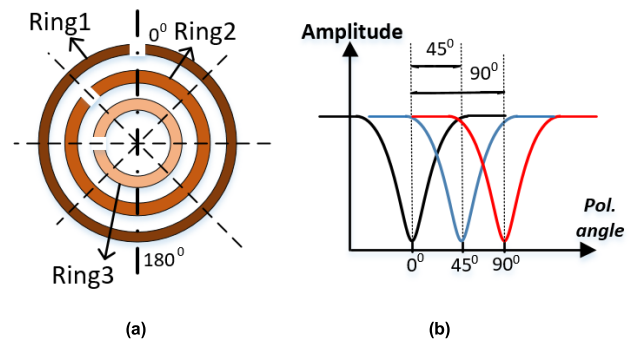


FIGURE 7. Encoding technique based on polarisation diversity [22] (a) the tag layout, and (b) the tag response.

the benefit of this compact size tag design was using a narrow frequency band for encoding data. The drawback of the tag was the complexity of reader to have a mechanical rotation of antenna in different angles. The tag had three resonators in size of  $3\text{cm} \times 3\text{cm}$ , and encoded with 6 bits of data in 3.4 to 7.1 GHz.

Furthermore, a compact dual polarised chipless RFID tag was proposed by Islam and Karmakar [23] using multiple-slots resonators on a rectangular patch antenna which produces 2 bits data in each frequency using vertical or horizontal polarisations. Resonators with the same polarisation were placed in separated patches to reduce mutual coupling. As an example, one tag with all “1”s in H- polarisation and two “0”s in V- polarisation are demonstrated in Fig. 8 with their frequency response in both polarisations. Although the adjacent resonators are separated in two arrangements, the coupling effect can still be seen in the form of a frequency shift in transition between 1 to 0. To improve this work, an 18 bit dual polarised in a compact size is proposed in [24] which used I slotted antenna patch in the frequency range of 7-13 GHz in which low RCS and short range detection are the weak points of the structure.

A similar dual polarised fully printed 3D stacked chipless RFID tag was reported by Preradovic [25] which used 2 sets of dipole antennas in both vertical and horizontal directions, and integrated the tag both in vertical and horizontal polarisations. This tag was printed on a low-cost polyimide thin film with screen-printing, which made it suitable for banknote chipless RFID tags. Moreover, the reading range for this tag was 20cm with an operating frequency of 1.8 to 3GHz.

### C. TIME-FREQUENCY-GROUP DELAY BASED CHIPLESS RFID TAGS

In most of the time-frequency-group delay based chipless RFID tags [26]–[30], microstrip C-section resonators were cascaded, and a dispersive delay structure (DDS) was constructed, which presents a frequency dependent time delay to the signal that travels through [4]. Since the input pulse was a combination of frequencies in the time domain, the received signal in a specific frequency would be delayed after passing through C-section. The amount of group delay could

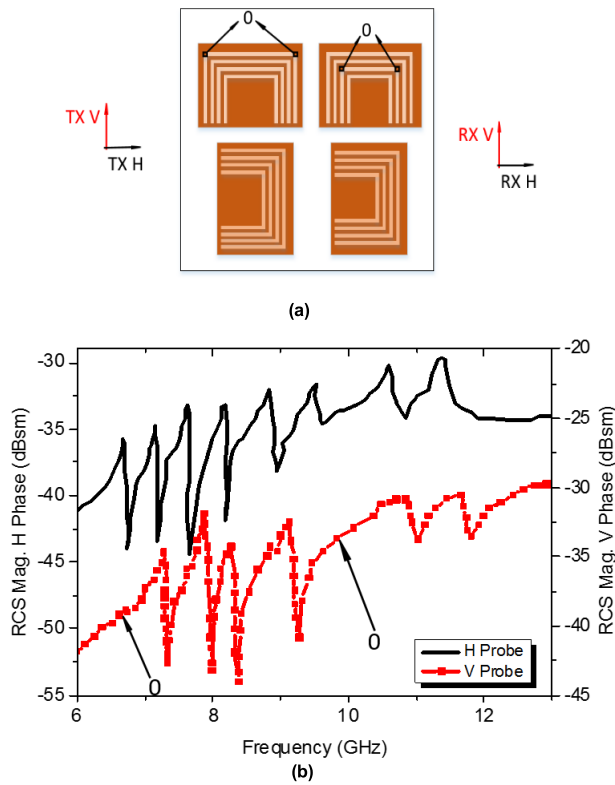


FIGURE 8. (a) 16-bit dual polarised tag with all 1 in H-polarization and two 0's in V-polarization and (b) frequency response [23].

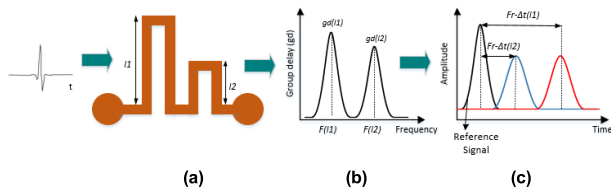


FIGURE 9. The principle of utilisation of group delay in the chipless tag. (a) structure of the proposed tag, (b) group delay curve in the frequency domain, and (c) corresponding time delay [28].

be controlled by changing the parameters of C-section. One approach to coding was changing group delay for a particular frequency by making a small change in the length of the C section, as shown in Fig. 9. In the case of having a significant amount of group delay, the corresponding bit can be bit “1” and having a small amount of group delay defined as bit “0” [26]–[28].

Another approach of encoding data is to use DDS to generate pulse position modulate integration signal [29], [30]. In this method, the integration signal should be a train of pulses at different frequencies, and by passing through the tag, each frequency will delay in a different value. In this coding a shift of frequency position of the pulse to the right side is considered as bit “1”, and a shift to left side represent bit “0”. Although by changing the group delay in each frequency, a high capacity of encoded data can be achieved in theory, there is a significant drawback for this method as

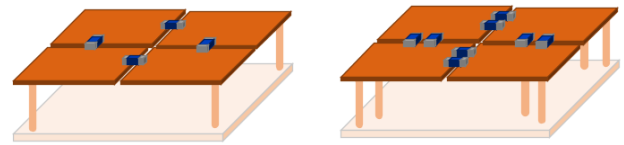


FIGURE 10. Prototype coding particles for group delay modulation with via inductor and two parallel via inductors and adapted SMD capacitance [31].

resonance frequency, and group delay cannot be controlled independently, and it creates ambiguity in signal processing.

In addition, a group delay modulation based on metamaterial concept with a stacked patch antenna was proposed in [31]. The frequency response of this tag varied by structure, the position of vias, number of parallel vias, and the number of lump element capacitors traversing the gap crossing the patch. The structure of this tag is shown in Fig. 10. The loaded quality factor of LC circuit, created by capacitor lump element and the capacitance gap on patch and inductance of via and patch, determine the group delay in each encoding particle. The main problem with this design is that group delay and frequency positions can not be controlled independently in the design. In addition, this structure is not fully planar and can not be printed as it contained via holes and SMD capacitors.

#### D. TIME-FREQUENCY NON-GROUP DELAY BASED CHIPLESS RFID TAGS

A time-frequency encoded chipless RFID tag with a reused frequency option is suggested in [32]. In this encoding technique, the tag consists of two receiving and transmitting tag antennas, one broadband power divider, a time delay circuit and two multi-resonators. The same frequency signature of the resonators can be generated in two time slots, by using the two delay meandered line, with different lengths. The tag ID can be extracted through time-frequency signal processing. The reflected signal from the tag, which was interrogated by a pulse, consisted of three pulses. They were transmitted pulse, the output of port #1 and port #2. By utilising time windowing, each output of ports could be separated in the time domain to detect the resonances in frequency domain. Therefore, for each frequency position, two states of data in the time domain could be achieved. For this structure, the operation frequency range was from 4 GHz to 6.5 GHz. Although this design is printable and has the potential for high data capacity, the large size of this tag design is a barrier in practical applications.

#### E. MODULATED ENCODED CHIPLESS RFID TAGS

One approach to increasing data capacity is to consider more than one parameters of the resonator which can be controlled independently. Recently some interesting research has been conducted to use features such as bandwidth or amplitude level or shape of RCS to encode data to the tag.

For example, one approach was considering notch bandwidth and frequency position, which could provide 4 bits of

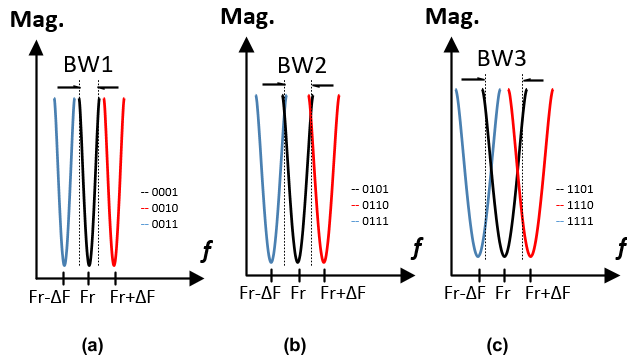


**FIGURE 11.** Basic principle for coding technique: (a) Codes for notch with bandwidth BW1, (b) Codes for notch with bandwidth BW2, and (c) Codes for notch with bandwidth BW3 [33].

data for each single resonators in [33]. The operating frequency was 2 to 5 GHz. In this encoding technique, the bandwidth of each resonance was controlled by three elements, and they were a dipole, a rectangular ring and rectangular patch elements that generate the first, the second and the third bandwidth as shown in Fig. 11. Moreover, the main challenge in this encoding technique was the tag ID detection. In order to estimate frequency bandwidth, a smart singular value decomposition technique was used.

Encoding information based on the magnitude level of RCS in depolarised chipless RFID tag was proposed for the first time by Rance and Siragusa [34]. In [35] information coding over magnitude level of RCS in addition to frequency position was presented. Single-layer tags based on C-folded dipoles are designed to have different magnitude levels. A magnitude span up to a 15.2 dB with a resolution of 3.5dB was achieved, and an additional scatter was used as a reference in RCS amplitude measurement. Due to coupling between resonators, the total code capacity was limited to 15 bits within a tag of size 3 cm × 4 cm. This tag design is an interesting option to be printed on paper as compared to frequency position-coded tags which have a low-quality factor of resonance in the paper substrate.

Furthermore, in [36], a hybrid chipless RFID tag was proposed utilising impedance loading. The principle of this structure is shown in Fig. 12. It can be seen that the resonances depth generated by ring resonators can be controlled by SMD loading resistors connected to each ring. Therefore, there was more than one state of data at each frequency position, which had the possibility of generating 23.7 bits of data in the size of 3cm × 3cm. The operating frequency of this design was 3 to 9 GHz. The drawback of this structure was the non-planar feature of the tag, as it was required to change the SMD resistors and via holes positions for varying the tag ID.

Another approach was using step impedance resonator to control fundamental resonance frequency as well as first harmonic frequency independently by changing impedance and length ratio which achieved  $2^{2N}$  bits using N resonators [37]. Moreover, a dual-band chipless RFID tag was presented

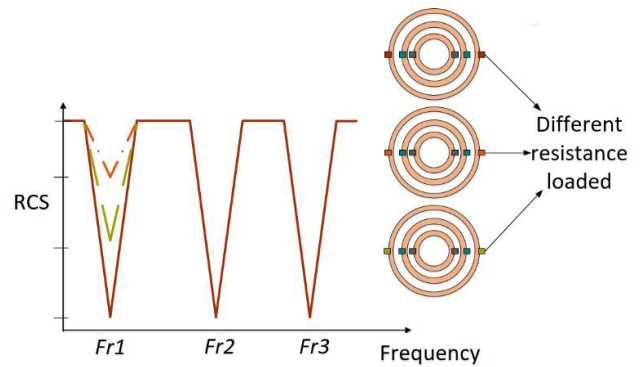


**FIGURE 12.** The coding principle of ASK [36].

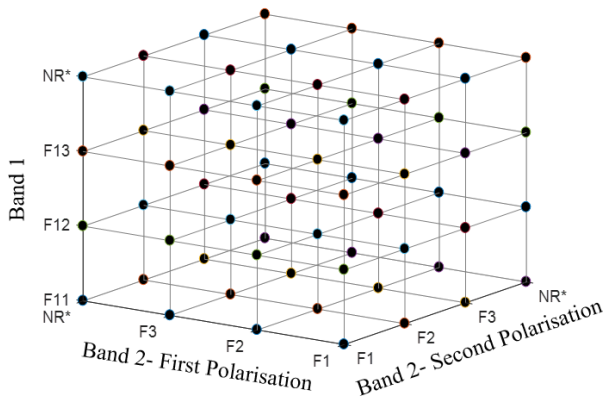
in [38] in which 3N bits could be achieved over each resonator.

An angle-based chipless RFID tag was proposed in [39] which was polarisation independent. Data were encoded by controlling space angle between two arms of V-shape scattered. Furthermore, by reforming the UIR into the SIR, the second harmonic of the scattered field was suppressed and the spectrum efficiency was improved. In this hybrid tag, 3bits of data could be encoded with each scattering. The operating frequency was 1.83 to 2.15GHz and identification errors were less than 3.9 degrees.

### III. A NOVEL THREE-DIMENSIONAL ENCODED CHIPLESS RFID TAG

As explained, the hybrid chipless RFID tags, which are proposed in the literature, mostly used two dimensions for data encoding. In order to increase the data capacity of chipless RFID tags, it is a novel solution to utilise more than two dimensions of encoding technique. In this paper a new hybrid chipless RFID tag with three dimensions of encoding technique is proposed in order to increase the data capacity. The three utilised dimensions are dual-band, polarisation diversity, and frequency division. This structure is a one-layer design, which can be printed on different materials such as plastic and paper as well as PCB fabrication. In addition to high data capacity of this tag in a limited bandwidth, the RCS level of this design is relatively high, which can enhance the reading ranges.

One of the crucial challenges in chipless RFID tag detection is the coupling effect between adjacent resonators in multi resonator structures [8], [40], which has caused difficulties in design, and detection. To address this issue, the number of active resonances in the bandwidth can be minimised and in fact, the other parameters of the resonator can be assigned for encoding. Moreover, functioning as a multi-resonator structure, multiple virtual resonators can be defined while only one physical resonator is available in the tag. Based on this idea, in this paper, a dual-band resonator with polarisation diversity, which generates at least 9 bits of data per resonator



\*NR: No resonance

FIGURE 13. The possible states of data for one resonator with 4-frequency division at each dimension (including no resonance).

with only two occupied frequency positions per each state, is proposed.

**A. DUAL BAND-POLARISATION DIVERSITY- FREQUENCY DIVISION ENCODING TECHNIQUE**

The proposed chipless RFID encoding technique uses a dual-band resonator which has polarisation diversity in the second band. Moreover, the frequency division technique is used for the resonances of both bands and both polarisations to minimise the number of the active resonators. Assume having a tag with  $K$  virtual resonators, and each of those resonators generates  $N$  states of data in the first dimension (first band) and  $M$  and  $L$  states in the second and third dimensions (second band in Y-polar and X-polar), the data capacity can be calculated from equation (1).

$$Data\ capacity = \log_2 \binom{K}{J} + J(\log_2^N + \log_2^M + \log_2^L + \log_2^K) \tag{1}$$

where

$K$  is the number of virtual resonators,  
 $J$  is the number of physical resonators,  
 $N$  is the number of states in the first band of each resonator,  
 $M$  is the number of states in the second band and Y-polar, and  
 $L$  is the number of states in the second band and X-polar.

It should be noticed that in the physical chipless RFID tag, only one of the designed virtual resonators is presented and the selection of that resonator can produce extra bits according to the number of available virtual resonators.

As an example by defining four states of data in frequency division for each frequency band and each polarisation, 6 bits of data can be achieved per resonator. These four states for each band and polarisation are generated by assigning three frequency positions for each resonance and one state to no resonance condition. The possible states of data for one resonator with 6 bits of data using three frequency positions at each band and polarisation are shown in Fig. 13. In this

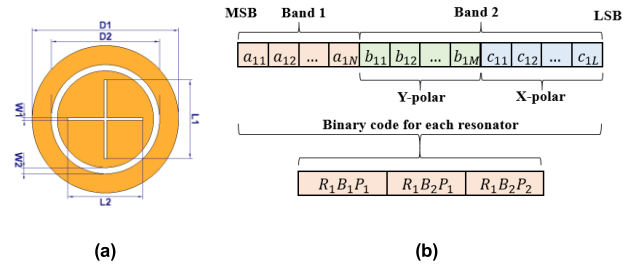


FIGURE 14. (a) A Dual-band tag resonator and (b) the bit stream of binary code for each resonator.

paper, in order to prove the concept, a chipless RFID tag with 9 bits per resonator was designed and fabricated.

**B. THE TAG STRUCTURE**

The proposed resonator for this hybrid chipless RFID tag is shown in Fig. 14 (a). This resonator is a circular shaped-antenna with a ring resonator slot and a plus-shaped slot with different lengths. The first resonance is generated by the slot ring resonator, which can be excited with vertical and horizontal polarisations with the orientation insensitive reflection. The cross-shaped slot generates the second band resonances. The vertical slot can be excited via vertical polarisation, and the horizontal section of the cross can be excited only by horizontal polarisation. Therefore, the polarisation diversity in co-polar RCS of the cross shape slot can generate two independent resonances in each perpendicular polarisation. The first-band resonance frequency position can be adjusted by changing the diameter,  $D2$ , and at the second band, the length of vertical and horizontal cross-shaped slot can tune the response frequencies in vertical and horizontal polarisations. The important thing in designing this tag is that the resonances at all three dimensions, each band or each polarisation can be tuned independently.

In addition the binary bit pattern for one resonator is shown in Fig. 14 (b) which illustrates that the bits related to the first band are the MSB and the bits encoded by the second band and the second polarisation are the LSB in the code. In this code  $R_i$  is corresponding to the index of a virtual resonator,  $B_i$  and  $P_i$  are describing the band and polarisation respectively. For example,  $R_1B_1P_1$  is corresponding to the bits generated from the first band resonances in the first polarisation of the resonator #1.

As it was mentioned in this encoding technique, in order to increase the spatial efficiency, only one physical resonator is available while multiple virtual resonators can be defined depending on the available frequency range. Therefore, in a multi virtual resonator, extra bits at MSB can be allocated to define the selection of one resonator out of  $K$  virtual resonators. For instance, when there are two virtual resonators available, only one bit is allocated to the resonator selection bit which can be 0 or 1. Moreover, since each virtual resonator has two frequency band resonances with polarisation diversity, there is a similar binary formation for each resonator.

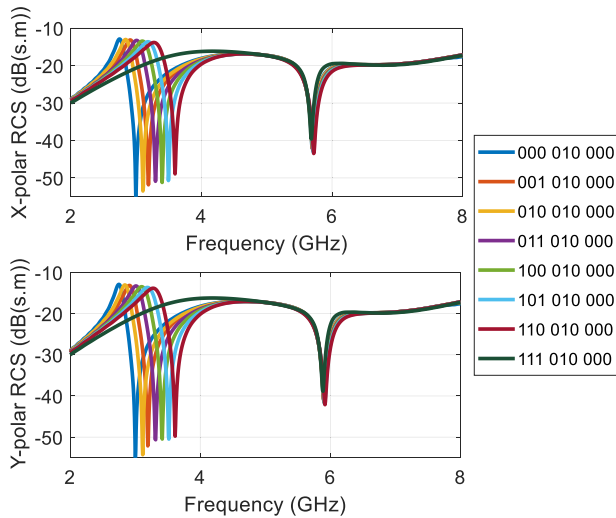


FIGURE 15. X-polar and Y-polar RCS in tag ID set 1, all combinations of the first band frequency division.

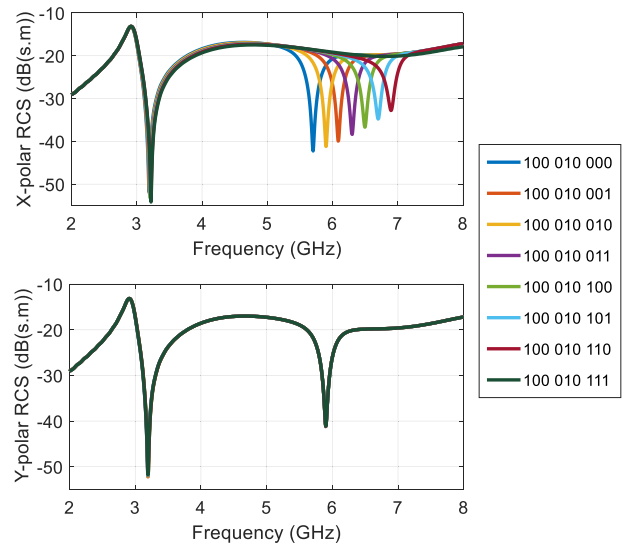


FIGURE 17. X-polar and Y-polar RCS in tag ID set 3, all combinations of the second band in X-axis frequency division.

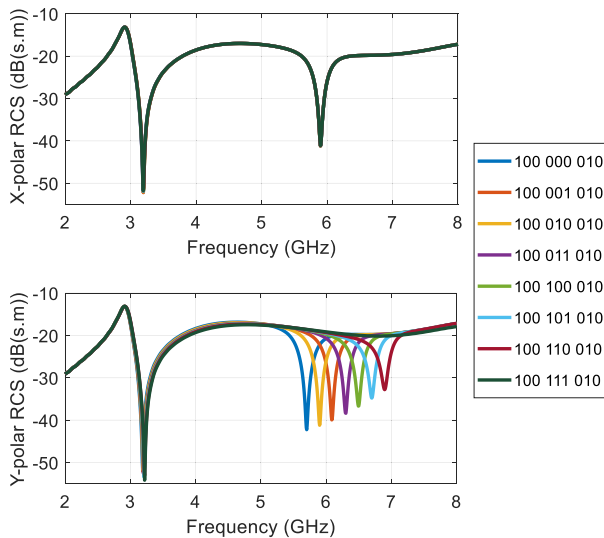


FIGURE 16. X-polar and Y-polar RCS in tag ID set 2, all combinations of the second band in Y-axis frequency division.

To prove the concept, a one-resonator chipless RFID with 8 frequency-division positions at each band and each polarisation is simulated and measured. In Figs. 15-17, different combinations of the 9-bit tag ID are depicted, which proves that the resonances at each band can be adjusted with the least coupling effect on the other resonance frequency position in the second band and second polarisation. This structure was simulated in CST Microwave Studio™, and Taconic Cer-10 substrate with 0.76 mm thickness, and permittivity of 10 were utilised.

As it can be seen in Fig. 15, the allocated bandwidth for the first band was 3 to 3.6 GHz with seven frequency positions, which can be tuned by changing the ring slot resonator radius. The data states, which are related to the presence of the resonance at any seven-frequency positions in addition to the absence of resonances in the first band, produce the first 3 bits

of encoded data. As it was expected, the first band resonance is independent to polarisation due to the symmetric shape. The other important point, which is shown in this figure, is that although the first band resonance shifted at different frequency point, the second band resonance stayed in the same position in both polarisations.

Furthermore, all combinations related to the second 3 bits which are related to the tuning of vertical slot length are shown in Fig. 16. The allocated bandwidth for the second band is 5.7 to 6.9 GHz with seven frequency positions and one state of no resonance. The length of the slot resonator changed from 4 to 5.94 mm to generate all eight states of data. In addition, it can be seen that the second band resonance in Y-polar has been shifted independently and the first band resonance and second band resonance at X-polar occurred at the same frequency position in all states. Similarly, in the third set of tag ID which corresponds to the last three bits of tag ID, the X-polar of the tag varied at each state. To generate eighth states, only the second band slot resonator length in X-polar was changed with no effect on other resonances in Y-polar and the first band, as shown in Fig. 17.

C. MEASUREMENT RESULTS

Using the proposed structure, a chipless RFID tag with a tag ID of 010001100 was designed and fabricated. A Taconic Cer-10 substrate with permittivity of 10 and a thickness of 0.76 mm was used for this design. In the layout of this design, the outer radius of the slot ring resonator,  $D_2$ , was 9.18 mm and the width of this slot,  $W_2$ , was 1mm. In the frequency signature, the resonance corresponding to this ring resonator was the first band resonance occurred at 3.2 GHz. Also, the length of the plus-shaped slot in X-axis and Y-axis were 12.4 mm and 11 mm, respectively, which produced the second band resonances at 5.9 GHz and 6.5 GHz in X-polar and Y-polar respectively. A photo of the fabricated tag is shown in Fig. 18.





**FIGURE 18.** The fabricated tag on Taconic Cer-10 that is corresponding to the tag ID 010001100. D2 = 9.18 mm, W2 = 0 mm, L1 = 12.4 mm, L2 = 11 mm, and W1 = 0.4 mm.



**FIGURE 19.** The tag measurement setup.

The tag frequency signature was measured in an ordinary lab environment as shown in Fig. 19, utilising a VNA model Anritsu 37247D and a Horn antenna. Since polarisation diversity was applied for data encoding, the RCS of the tag should be measured in both X-polar and Y-polar. Therefore, two approaches can be implemented for this measurement setup. The first one was using two horn antennas with perpendicular polarisations. The second approach was having only one antenna which can be mechanically rotated 90 degrees for the measurement of the X-polar or Y-polar RCS. In addition to simplifying the measurement, the antenna orientation can be fixed for a specific polarisation, and the tag can be placed in front of the antenna in two angles for X-polar or Y-polar measurement. For this lab measurement with a fixed antenna position, the tag was placed with two perpendicular orientations corresponding to both of the polarisations.

In this measurement, a background subtraction technique was used to reduce the effect of the environment in the tag RCS. In the background subtraction technique, the first step is to measure the  $S_{11No-Tag}$  of the antenna in the absence of the tag, which includes the loading effect of the environment. Secondly, the tag should be placed in front of the antenna, and the  $S_{11Tag}$  is measured. This measured vector consists of the environment loading effect, the antenna response and the reflection from the chipless RFID tag. The RCS of the tag can be calculated by removing the loading effect of the environment using formula (2).

$$\text{Tag Frequency Signature} = S_{11Tag} - S_{11No-Tag} \quad (2)$$

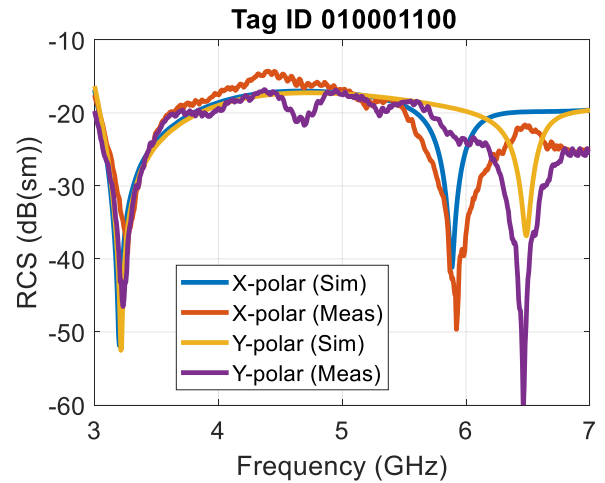


**FIGURE 20.** The simulation and measurement results for the tag ID 010001100.

This background subtracting procedure was applied in both stages of the tag measurement (measuring the X-polar and Y-polar RCS).

The measured frequency response in both X-polar and Y-polar is compared to the simulation results in Fig. 20. It can be seen that the first band resonance has the same frequency position (3.2GHz) in both X-polar and Y-polar measurement as well as the simulation results. Moreover, the second band resonances were tuned independently to 5.9 GHz and 6.5 GHz in X-polar and Y-polar respectively, and the results of measurement agreed with the simulation results.

This measurement result proves the excellent performance of the tag as a three-dimensional encoded chipless RFID tag, which contains 9 bits of data in one resonator. It also can be seen that the maximum RCS level of measured frequency signature was around -15 dB and the depth of nulls was more than 30 dB. These two values are excellent in terms of high level of RCS that can help in increasing the reading range.

#### D. DISCUSSIONS

A suitable chipless RFID tag for practical applications should yield high data capacity, high RCS, the least coupling effect between adjacent resonators, and the least effect of transition between binary states ‘1’ to ‘0’ (or vice versa). Moreover, reducing the size of the tag and minimizing the occupied frequency bandwidth are preferred to simplifying the reader architecture. Moreover, it is desired to have a planar printable structure to reduce the cost and complexity of fabrication. An important factor for designing the tag is the level of complexity of the tag ID detection algorithm, which is related to the data encoding technique. In hybrid chipless RFID tags, more than two aspects or dimensions of data encoding are used in order to increase data capacity.

As it was discussed in previous sections, hybrid chipless RFID tags were classified into four groups based on different data encoding techniques. The common thing in reported

**TABLE 1.** Comparison analysis of hybrid chipless RFID tags.

Reference	Method of data encoding	Number of bits per resonators	Number of layers	Number bits per $cm^2$	Number bits per $\lambda_c^2(cm^2)$	Frequency (GHz)
[17]	Frequency-phase	4.58	1	2.86	1.43	2.5-7.5
[18]	Phase-frequency	1	2	0.022	0.022	2.1-2.6
[22]	Polarization- Frequency	2	1	0.66	0.33	3.4- 7.1
[23]	Polarization- Frequency	2	1	5.22	2.5	6-12
[24]	Polarization- Frequency	2	1	4.08	3.4	7-13
[32]	Time- frequency (non-group delay)	2	2	0.14	0.32	4- 6
[33]	BW division	4	1	3.6	2	2-5
[35]	RCS level-frequency	3	1	1.25	0.41	2-5
[36]	Resonance depth- frequency	7.9	2 (Non-planar)	2.63	2.13	3-9
<b>This work</b>	<b>Dual-band, polarization diversity-frequency division</b>	<b>9</b>	<b>1</b>	<b>1.56</b>	<b>0.486</b>	<b>3-3.6 and 5.7-6.9</b>

hybrid tags is that for all structure, two parameters of each resonator contain the encoded data. This investigation led to discovering a research gap to design a chipless RFID tag that can include three dimensions or parameters for encoding data. Utilizing three parameters of one resonator can increase the data capacity and reduce the size of the tag significantly. In multi-dimensional encoding techniques, a serious challenge is to control three various parameters of a passive resonator independently with the least coupling effect.

In this paper, a three-dimensional encoding technique for a hybrid chipless RFID tag is proposed. Dual-band, polarisation diversity in the second band and frequency division multiplexing are used to increase data capacity. By defining the high resolution of frequency division for this technique and using the other two dimensions of the encoding technique, high data capacity per resonator can be achieved.

In order to compare the performances of different hybrid chipless RFID tag designs in the open literature and the proposed structure, Table 1 provides a comparative analysis. It can be seen that the three works have the highest data capacity among those on the list. The first one is the proposed structure by the authors in this paper by using three-dimensional encoding techniques, which produce 9 bits of data per each resonator with a printable structure that can be printed on different materials such as plastic and paper. The second one uses the resonance depth and frequency position [36] for encoding data, and generates 7.9 bits per resonator, while there is a drawback of having a non-planar structure in which assembling SMD resistors is required. In addition, the frequency-phase bandwidth technique [17] produces 4.58 bits per resonator which has a planar structure and high RCS.

Furthermore, regarding spatial efficiency, the number of bits per  $cm^2$ , and the number of bit per  $\lambda^2$  are provided. To calculate the wavelength, the smallest value of wavelength in the frequency range is considered. Regardless of the effect of the frequency range, the polarization-frequency techniques presented in [23] and [24] have the highest value while they produce only two bits of data per resonator. The next designs with efficient design regarding to size are a bandwidth division technique in [33] and a phase frequency encoding in [17] with the spatial efficiency of 3.6 and 2.86 respectively. In addition, the Resonance depth- frequency method in [36], has a spatial efficiency of 2.63 while the non-planar structure is the drawback. The structure proposed in this paper also has an efficiency factor of 1.56. Other reported hybrid chipless RFID tags in the table have a lower value of spatial efficiency (ranging from 1.2 to 0.02).

Moreover, in comparison with the spatial efficiency in term of bits per  $\lambda_c^2$ , which is the number of bits per square of the shortest wavelength in cm, the Polarization-Frequency [23], [24] and Resonance depth- frequency [36], and BW division [33] techniques with 3.4, 2.5, 2.13, and 2 bits per  $\lambda_c^2(in cm^2)$  respectively had the highest spatial efficiency. The next efficient encoding techniques were Frequency-phase [17] and Dual-band, polarization diversity-frequency division technique by authors with 1.43 and 0.486 spatial efficiency respectively.

As a conclusion, the proposed structure in this paper has a high number of bit per resonator as compared to the other reported tags in Table 1. In addition, this one-resonator-tag occupied 600 MHz in the first band and 1200MHz in the second band. In the case of increasing the number of virtual resonators, the spatial efficiency can increase significantly. For instance, having two virtual resonators that can produce

10 bits of data based on the proposed three-dimensional encoding technique, and considering one additional bit for selection of the physical resonator, 11 bits of data per resonator can be achieved.

#### IV. CONCLUSIONS

In this paper, a summary of recent research on the improvement of hybrid chipless RFID was provided. Since hybrid chipless RFID is a new technique in chipless RFID field, only a few works were reported. All reported encoding techniques were based on only two dimensions which are frequency and polarisation. Although these approaches have increased encoding data capacity in a compact size as compared to one-dimensional chipless RFID tags, they have limitations in data capacity per element, tag detection algorithm, and reading range. These are significant challenges in practical applications. Therefore, a novel hybrid chipless RFID tag with higher encoding data capacity is required. Three dimensions of encoding can increase the data capacity, and reduce the size of the tag significantly.

Moreover, in order to utilise a hybrid chipless RFID tag for industrial application, besides the data capacity, the design should fulfil other specifications such as efficient data decoding techniques, and frequency reuse using diversity techniques. Therefore, a three-dimensional encoding technique was proposed in this paper, which has paved the way forward to the EPC Global standard for chipless RFID systems. In the proposed tag, utilising polarisation diversity of a dual-band resonator and applying a frequency division technique could increase the data capacity to at least 9 bits per resonator. Furthermore, the high level of RCS for this tag could enhance the reading range. The results of the measurement of the proposed tag agreed with the simulation result, which showed the excellent performance of this structure.

#### REFERENCES

- [1] K. Finkenzeller, *RFID Handbook: Fundamentals and Applications in Contactless Smart Cards and Identification*, 2nd ed. Chichester, U.K.: Wiley, 2003.
- [2] S. Preradovic and N. C. Karmakar, "Chipless RFID: Bar code of the future," *IEEE Microw. Mag.*, vol. 11, no. 7, pp. 87–97, Dec. 2010.
- [3] M. Forouzandeh and N. Karmakar, "Chipless RFID tags and sensors: A review on time-domain techniques," *Wireless Power Transf.*, vol. 2, pp. 62–77, 2015.
- [4] N. C. Karmakar, R. Koswatta, P. Kalansuriya, and R. E-Azim, *Chipless RFID Reader Architecture*. Boston, MA, USA: Artech House, 2013.
- [5] D. Girbau, A. Lázaro, and A. Ramos, "Time-coded chipless RFID tags: Design, characterization and application," in *Proc. IEEE Int. Conf. RFID-Technol. Appl.*, Nov. 2012, pp. 12–17.
- [6] C. Herrojo, J. Mata-Contreras, A. Núñez, F. Paredes, E. Ramon, and F. Martín, "Near-field chipless-RFID system with high data capacity for security and authentication applications," *IEEE Trans. Microw. Theory Techn.*, vol. 65, no. 12, pp. 5298–5308, Dec. 2017.
- [7] M. A. Riaz, H. Shahid, S. Z. Aslam, Y. Amin, A. Akram, and H. Tenhunen, "Novel T-shaped resonator based chipless RFID tag," *IEICE Electron. Express*, vol. 14, no. 18, p. 0728, 2017.
- [8] M. Polivka, J. Havlicek, M. Svanda, and J. Machac, "Improvement in robustness and recognizability of RCS response of U-shaped strip-based chipless RFID tags," *IEEE Antennas Wireless Propag. Lett.*, vol. 15, pp. 2000–2003, 2016.
- [9] M. Zomorodi and N. C. Karmakar, "On the application of the EM-imaging for chipless RFID tags," *Wireless Power Transf.*, vol. 2, no. 2, pp. 86–96, 2015.
- [10] M. S. A. Bhuiyan, "Toward EPC global chipless RFID tag design," M.S. thesis, Elect. Comput. Syst. Eng., Monash Univ., Melbourne, VIC, Canada, 2014.
- [11] T. Kim, U. Kim, J. Kwon, and J. Choi, "Design of a novel chipless RFID tag using a simple bandstop resonator," in *Proc. Asia-Pacific Microw. Conf.*, Dec. 2010, pp. 2264–2267.
- [12] G. A. Casula, G. Montisci, P. Maxia, and G. Mazzarella, "A narrowband chipless multiresonator tag for UHF RFID," *J. Electromagn. Waves Appl.*, vol. 28, no. 2, pp. 214–227, 2014.
- [13] O. Necibi, S. Beldi, and A. Gharsallah, "Design of a chipless RFID tag using cascaded and parallel spiral resonators at 30 GHz," presented at the 2nd World Symp. Web Appl. Netw. (WSWAN), Mar. 2015.
- [14] S. Preradovic, S. Roy, and N. Karmakar, "Fully printable multi-bit chipless RFID transponder on flexible laminate," in *Proc. Asia-Pacific Microw. Conf.*, Dec. 2009, pp. 2371–2374.
- [15] C. Herrojo, J. Naqui, F. Paredes, and F. Martín, "Spectral signature barcodes based on S-shaped split ring resonators (S-SRRs)," *EPJ Appl. Metamater.*, vol. 3, p. 1, Jun. 2016.
- [16] C. M. Nijās *et al.*, "Chipless RFID tag using multiple microstrip open stub resonators," *IEEE Trans. Antennas Propag.*, vol. 60, no. 9, pp. 4429–4432, Sep. 2012.
- [17] A. Vena, E. Perret, and S. Tedjini, "Chipless RFID tag using hybrid coding technique," *IEEE Trans. Microw. Theory Techn.*, vol. 59, no. 12, pp. 3356–3364, Dec. 2011.
- [18] I. Balbin and N. C. Karmakar, "Phase-encoded chipless RFID transponder for large-scale low-cost applications," *IEEE Microw. Wireless Compon. Lett.*, vol. 19, no. 8, pp. 509–511, Aug. 2009.
- [19] S. Majidifar, A. Ahmadi, O. Sadeghi-Fathabadi, and M. Ahmadi, "A novel phase coding method in chipless RFID systems," *AEUE-Int. J. Electron. Commun.*, vol. 69, pp. 974–980, Jul. 2015.
- [20] A. Vena, E. Perret, and S. Tedjini, "RFID chipless tag based on multiple phase shifters," in *IEEE MTT-S Int. Microw. Symp. Dig.*, Jun. 2011, pp. 1–4.
- [21] S. Genovesi, F. Costa, A. Monorchio, and G. Manara, "Chipless RFID tag exploiting multifrequency delta-phase quantization encoding," *IEEE Antennas Wireless Propag. Lett.*, vol. 15, pp. 738–741, 2015.
- [22] A. Vena, E. Perret, and S. Tedjini, "A compact chipless RFID tag using polarization diversity for encoding and sensing," in *Proc. IEEE Int. Conf. RFID*, Apr. 2012, pp. 191–197.
- [23] M. A. Islam and N. C. Karmakar, "A novel compact printable dual-polarized chipless RFID system," *IEEE Trans. Microw. Theory Techn.*, vol. 60, no. 7, pp. 2142–2151, Jul. 2012.
- [24] M. A. Islam and N. C. Karmakar, "Compact printable chipless RFID systems," *IEEE Trans. Microw. Theory Techn.*, vol. 63, no. 11, pp. 3785–3793, Nov. 2015.
- [25] S. Preradovic, "Printed 3D stacked chipless RFID tag with spectral and polarization encoding," *Microw. J.*, vol. 59, no. 4, pp. 122–132, 2016.
- [26] R. Nair, E. Perret, and S. Tedjini, "Novel encoding in chipless RFID using group delay characteristics," in *Proc. SBMO/IEEE MTT-S Int. Microw. Optoelectron. Conf. (IMOC)*, Oct. 2011, pp. 896–900.
- [27] R. Nair, E. Perret, and S. Tedjini, "Temporal multi-frequency encoding technique for chipless RFID applications," in *IEEE MTT-S Int. Microw. Symp. Dig.*, Jun. 2012, pp. 1–3.
- [28] R. Nair, E. Perret, and S. Tedjini, "Chipless RFID based on group delay encoding," in *Proc. IEEE Int. Conf. RFID-Technol. Appl. (RFID-TA)*, Sep. 2011, pp. 214–218.
- [29] S. Gupta, B. Nikfal, and C. Caloz, "RFID system based on pulse-position modulation using group delay engineered microwave C-sections," in *Proc. Asia-Pacific Microw. Conf.*, Dec. 2010, pp. 203–206.
- [30] S. Gupta, B. Nikfal, and C. Caloz, "Chipless RFID system based on group delay engineered dispersive delay structures," *IEEE Antennas Wireless Propag. Lett.*, vol. 10, pp. 1366–1368, Oct. 2011.
- [31] C. Mandel, B. Kubina, M. Schussler, and J. Jakoby, "Group-delay modulation with metamaterial-inspired coding particles for passive chipless RFID," in *Proc. IEEE Int. Conf. RFID-Technol. Appl. (RFID-TA)*, Nov. 2012, pp. 1–5.
- [32] M. S. Bhuiyan, R. E. Azim, and N. Karmakar, "A novel frequency reused based ID generation circuit for chipless RFID applications," in *Proc. Asia-Pacific Microw. Conf.*, Dec. 2011, pp. 1470–1473.

- [33] A. El-Awamry, M. Khaliel, A. Fawky, M. El-Hadidy, and T. Kaiser, "Novel notch modulation algorithm for enhancing the chipless RFID tags coding capacity," presented at the IEEE Int. Conf. RFID, Apr. 2015.
- [34] O. Rance, R. Siragusa, P. Lemaître-Auger, and E. Perret, "RCS magnitude coding for chipless RFID based on depolarizing tag," in *IEEE MTT-S Int. Microw. Symp. Dig.*, May 2015, pp. 1–4.
- [35] O. Rance, R. Siragusa, P. Lemaître-Auger, and E. Perret, "Toward RCS magnitude level coding for chipless RFID," *IEEE Trans. Microw. Theory Techn.*, vol. 64, no. 7, pp. 2315–2325, Jul. 2016.
- [36] Y.-Z. Ni, X.-D. Huang, Y.-P. Lv, and C.-H. Cheng, "Hybrid coding chipless tag based on impedance loading," *IET Microw., Antennas Propag.*, vol. 11, no. 10, pp. 1325–1331, 2017.
- [37] C. M. Nijas *et al.*, "Low-cost multiple-bit encoded chipless RFID tag using stepped impedance resonator," *IEEE Trans. Antennas Propag.*, vol. 62, no. 9, pp. 4762–4770, Sep. 2014.
- [38] D. Girbau, J. Lorenzo, A. Lazaro, C. Ferrater, and R. Villarino, "Frequency-coded chipless RFID tag based on dual-band resonators," *IEEE Antennas Wireless Propag. Lett.*, vol. 11, pp. 126–128, 2012.
- [39] C. Feng, W. Zhang, L. Li, L. Han, X. Chen, and R. Ma, "Angle-based chipless RFID tag with high capacity and insensitivity to polarization," *IEEE Trans. Antennas Propag.*, vol. 63, no. 4, pp. 1789–1797, Apr. 2015.
- [40] J. Havlicek, M. Svanda, M. Polivka, J. Machac, and J. Kracek, "Chipless RFID tag based on electrically small spiral capacitively loaded dipole," *IEEE Antennas Wireless Propag. Lett.*, vol. 16, pp. 3051–3054, 2017.



**FATEMEH BABAEIAN** received the B.S. degree in electrical engineering from Shiraz University, Shiraz, Iran, in 2010, and the M.S. degree in electrical engineering (Telecommunication) from the Amirkabir University of Technology, Tehran, Iran, in 2013. She is currently pursuing the Ph.D. degree in electrical engineering with Monash University, Australia. Her research interest includes chipless RFID, microwave, antenna array synthesis, and signal processing.



**NEMAI CHANDRA KARMAKAR** (S'91–M'91–SM'99) received the M.Sc. degree in electrical engineering from the University of Saskatchewan, Saskatoon, SK, Canada, in 1991, and the Ph.D. degree from the University of Queensland, Brisbane, QLD, Australia, in 1999. He has over 20 years of teaching, design, and development experience in antennas, microwave active and passive circuits, and RFIDs in Canada, Australia, and Singapore. He is currently an Associate Professor with the Department of Electrical and Computer Systems Engineering, Monash University, Melbourne, VIC, Australia. He has authored or co-authored over 220 referred journal and conference papers, 24 book chapters, and eight books. He holds nine international patent applications on chipless RFID.

• • •